

The Electrical Breakdown and Permeability Control of a Bilayer-Corked Capsule Membrane in an External Electric Field^{1,2}

Yoshio Okahata,* Satoshi Hachiya, Katsuhiko Ariga, and Takahiro Seki

Contribution from the Department of Polymer Chemistry, Tokyo Institute of Technology, Ookayama, Meguro-ku, Tokyo 152, Japan. Received August 28, 1985

Abstract: A large ultrathin nylon capsule (diameter 2 mm; membrane thickness 1 μm) whose porous membrane was corked with synthetic bilayers was prepared, and the permeability across the membrane was investigated under an external electric field. Permeation of NaCl, glucose, and water-soluble dyes stored in the inner aqueous core of the capsule was enhanced 5–176 times under a 20–80-V electric field, relative to that in the absence of the electric field. When the electric field ceased even after a long charging duration (3–5 min), the permeability reduced to the original slow rate. This permeability control could be reproduced repeatedly without damaging either corking bilayers or nylon capsule membranes. The electrically induced permeability enhancement was exponentially increased with increasing electric field in the range of 0–80 V. This could be explained by the reversible electrical breakdown of the corking bilayer which acts as a capacitor because of its poor conductivity under an electric field, and the transmembrane potential could produce transient pores in lipid bilayers. The extent of the electrically induced permeability enhancement depended on the conductivity of corking bilayers, the molecule size of permeants, and the ionic strength of both the inner and outer aqueous phases.

Transmembrane potentials are believed to play a major role in biological processes. When the membrane potential exceeds a threshold value, a local electrical breakdown (a formation of transient pores) seems to occur in lipid bilayers, allowing rapid passage of large substances and particles (up to the size of genes) which cannot normally permeate through the membrane.^{3,4} Extensive pulsation experiments of transmembrane potentials have been concluded on such convenient models as suspensions of liposomes⁵ and planner lipid bilayer membranes.^{6,7} However, in contrast to biological membranes, in the case of these artificial lipid bilayer membranes it has been impossible to induce stable transient pores which have not been accompanied by mechanical rupture of the membrane for any long duration (>1 s) by the electric field.

Recently we prepared a large, ultrathin, bilayer-corked capsule membrane in which the porous nylon membrane is corked with multilamellar bilayers.^{8–17} The capsule has both advantages of physically strong nylon capsule and characteristics of lipid bilayer vesicles. Permeation of water-soluble substances stored in the inner aqueous core of the capsule was reversibly controlled by stimuli

from outside such as temperature,^{8–10,17} photoirradiation,¹¹ ultrasonic power,¹² pH changes,^{13,14} and interactions with divalent cations.^{14–16} Their signal-receptive permeability control is explained by changes in the physical state of the corking bilayers which act as a "valve". Liposomal membranes could not achieve such a reversible permeability control because of their easily breakable lipid bilayer walls.

We report here that the permeability of the bilayer-corked capsule membrane can be reversibly regulated by an external electric field due to a breakdown of the corking bilayer by the transmembrane potential. The permeation mechanism with or without the electric field is discussed with respect to (i) the head group charge of lipid bilayers, (ii) the molecular size of permeants, (iii) the conductivity of lipid bilayers, (iv) the effect of the ionic strength of the aqueous phase, and (v) the activation energy data of permeation obtained from Arrhenius plots.

A schematic representation of the capsule and the apparatus for charging the external electric field are shown in Figure 1.

Experimental Section

Materials. Preparations of bilayer-forming amphiphiles, dialkyldimethylammonium bromide ($2\text{C}_n\text{N}^+ 2\text{C}_1$, $n = 12, 14, 16, 18$),⁸ sodium didodecylphosphate ($2\text{C}_{12}\text{PO}_4^-$),⁹ and 1,3-dihexadecyl-*rac*-glycero-2-phosphocholine ($2\text{C}_{16}\text{PC}$)¹⁴ were reported elsewhere. 4-[*p*-Dibutylamino]styryl]-1-methylpyridinium bromide (di-4-ASP) was prepared from *p*-(dibutylamino)benzaldehyde (11.7 g, 0.05 mol) and 4-picolinium bromide (9.4 g, 0.05 mol) in the presence of pyrrolidine (3.6 g) in refluxing ethanol according to the literature procedure:¹⁸ deeply colored red crystals (16.6 g, 82%), mp 214–216 °C. Liquid crystalline type, bilayer-forming amphiphiles, $\text{C}_{12}\text{-BB-C}_4\text{-N}^+$ and $\text{C}_{12}\text{-Azo-C}_4\text{-N}^+$, were prepared by the method described previously:²² mp 89 \rightarrow 120 °C and 122 \rightarrow 150 °C (arrows show a thermotropic liquid crystalline behavior), respectively.

Preparations of water-soluble permeants of a nonionic probe, 2,6-bis(quinamidomethyl)naphthalene (1), and a zwitterionic naphthalene probe, 2,6-bis(sulfopropyl)(*N,N*-dimethylammonio)methylnaphthalene (2), were reported elsewhere.¹⁰ Anionic water-soluble naphthalene probes, sodium naphthalen-1-sulfonate (3), disodium naphthalene-1,5-disulfonate (4), trisodium naphthalene-1,3,6-trisulfonate (5), and tetrasodium pyrene-1,3,6,8-tetrakisulfonate (6), were purchased commercially

(1) Functional Capsule Membranes. Part 22. Part 21: Seki, T.; Okahata, Y. *J. Polym. Sci., Polym. Chem. Ed.* **1986**, *24*, 61. For a review of this series, see: Okahata, Y. *Acc. Chem. Res.*, in press.

(2) Preliminary report: Okahata, Y.; Hachiya, S.; Seki, T. *J. Chem. Soc., Chem. Commun.* **1984**, 1377.

(3) (a) Zimmermann, U.; Shultz, J.; Pilwat, G. *Biophys. J.* **1973**, *13*, 1005. (b) Zimmermann, U.; Vienken, J.; Pilwat, G. *Bioelectrochem. Bioenerg.* **1980**, *7*, 554.

(4) Zimmermann, U.; Scheurich, P.; Pilwat, G.; Benz, R. *Angew. Chem., Int. Ed. Engl.* **1981**, *20*, 325.

(5) Teissie, J.; Tsong, T. Y. *Biochemistry* **1981**, *20*, 1548.

(6) Bhowmik, B. B.; Nandy, P. *Chem. Phys. Lipids* **1983**, *34*, 101.

(7) Chernomordik, L. V.; Sukharev, S. I.; Abidor, I. G.; Chizmadzhev, Yu. A. *Biochim. Biophys. Acta* **1983**, *736*, 203.

(8) Okahata, Y.; Lim, H.-J.; Nakamura, J.; Hachiya, S. *J. Am. Chem. Soc.* **1983**, *105*, 4855. Okahata, Y.; Hachiya, S.; Nakamura, G. *Chem. Lett.* **1982**, 1719.

(9) Okahata, Y.; Lim, H.-J.; Hachiya, S.; Nakamura, G. *J. Membr. Sci.* **1984**, *19*, 237.

(10) Okahata, Y.; Iizuka, N.; Nakamura, G.; Seki, T. *J. Chem. Soc., Perkin Trans. 2*, **1985**, 1591.

(11) Okahata, Y.; Lim, H.-J.; Hachiya, S. *J. Chem. Soc., Perkin Trans. 2* **1984**, 989; *Makromol. Chem. Rapid Commun.* **1983**, *4*, 303.

(12) Okahata, Y.; Noguchi, H. *Chem. Lett.* **1983**, 1517.

(13) Okahata, Y.; Seki, T. *J. Am. Chem. Soc.* **1984**, *106*, 8065; *Chem. Lett.* **1984**, 1251.

(14) Okahata, Y.; Seki, T. *J. Microencap.* **1985**, *2*, 13.

(15) Okahata, Y.; Lim, H.-J. *J. Am. Chem. Soc.* **1984**, *106*, 4696.

(16) Okahata, Y.; Lim, H.-J.; Nakamura, G. *Chem. Lett.* **1983**, 755.

(17) Okahata, Y.; Noguchi, H.; Seki, T. *J. Membr. Sci.* **1985**, *24*, 168.

Okahata, Y.; Nakamura, G.; Nachiya, S.; Noguchi, H.; Lim, H.-J. *J. Chem. Soc., Chem. Commun.* **1983**, 1206.

(18) Hassner, A.; Birnbaum, D.; Loew, L. M. *J. Org. Chem.* **1984**, *49*, 2546. Loew, L. M. *J. Biochem. Biophys. Methods* **1982**, *6*, 243.

(19) Okahata, Y.; Ando, R.; Kunitake, T. *Ber. Bunsenges. Phys. Chem.* **1981**, *85*, 789.

(20) Loew, L. M.; Scully, S.; Simpson, L.; Waggoner, A. S. *Nature (London)* **1979**, *281*, 497.

(21) Loew, L. M.; Simpson, L.; Hassner, A.; Alexanian, V. *J. Am. Chem. Soc.* **1979**, *101*, 5439.

(22) Kunitake, T.; Okahata, Y.; Shimomura, M.; Yasunami, S.; Takarabe, K. *J. Am. Chem. Soc.* **1981**, *103*, 5401.

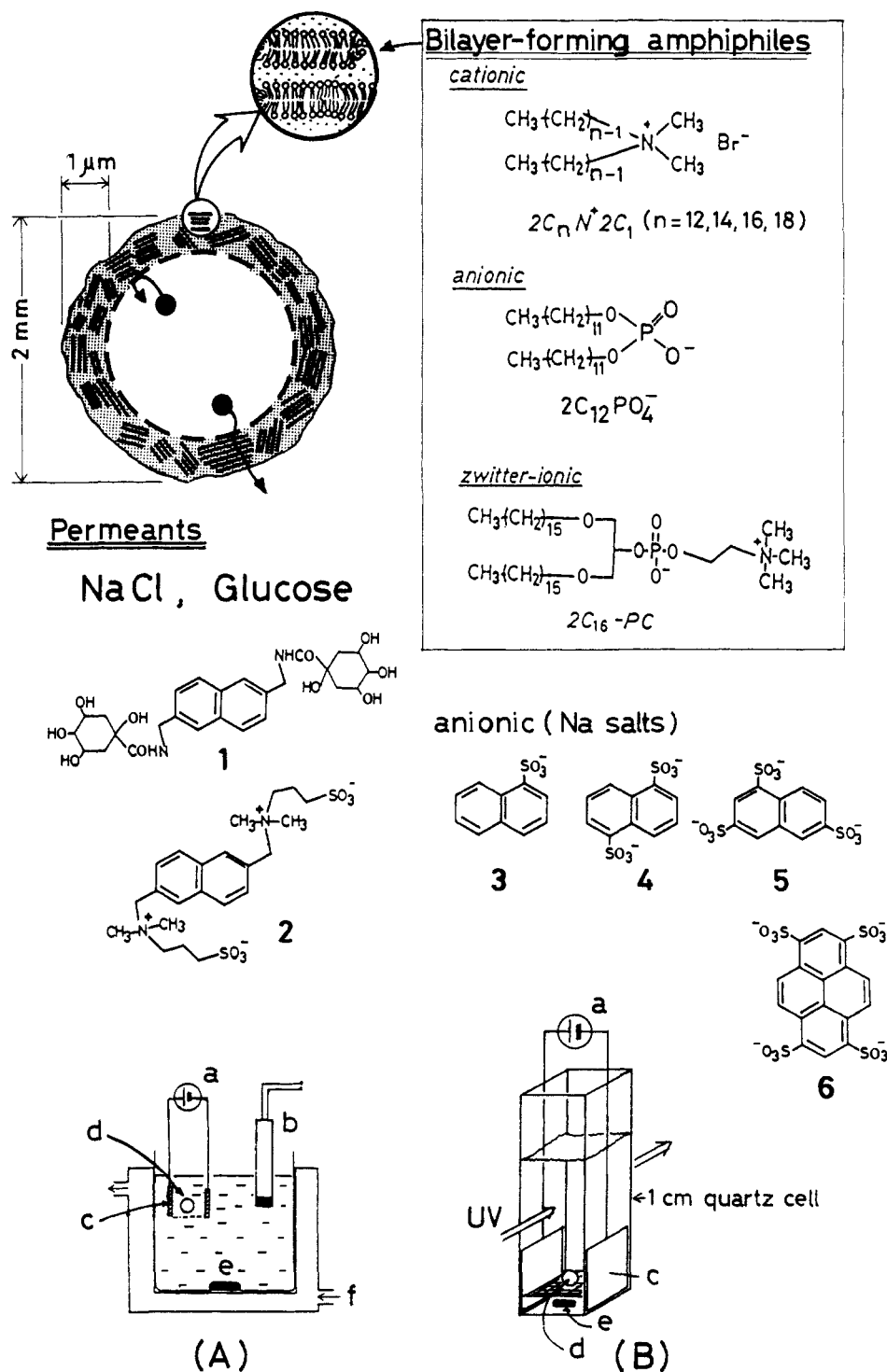


Figure 1. Schematic illustrations of a bilayer-corked capsule membrane and apparatuses for permeation experiments under an external electric field. The apparatuses A and B were used for the NaCl and glucose permeation and the dye permeation, respectively: (a) High voltage power supply (dc 0–300 V); (b) detector (conductance cell for the NaCl permeation or H_2O_2 electrode covered with a GOD film for the glucose permeation); (c) Pt electrode (area 1 cm \times 1 cm, separation between the two electrodes 1 cm); (d) the bilayer-corked capsule membrane; (e) stirring rod; (f) thermostated circulating water.

(Tokyo Kasei Co., Japan) and were further purified by recrystallization from aqueous acetone.

Preparation of Capsules. Large nylon-2,12 capsules (diameter 2 mm; membrane thickness 1 μm) were prepared from ethylenediamine and 1,10-bis(chlorocarbonyl)decane by interfacial polycondensation by the method previously described.^{8–17} The obtained capsules having a porous nylon membrane were dialysed against 0.2 M NaCl, 0.5 M glucose, or 0.001 M water-soluble dyes to give capsules containing the respective probe molecule inside.

Amphiphile-corked capsules were prepared as follows.^{8–17} Twenty pieces of the capsule-containing permeants in the inner aqueous core were transferred to a hot dodecane solution (3 ml) of dialkyl amphiphiles (20

mg) and maintained at 60 $^\circ\text{C}$ for 5 min. After being cooled, the amphiphiles were precipitated spontaneously as multiple bilayers at the interfacial, porous capsule membrane between the inner aqueous phase and the outer dodecane solution. The amphiphile content was $20 \pm 3 \mu\text{g}$ per capsule, and dodecane was confirmed by elemental analysis not to be an impurity (less than 5 wt%) in the corking bilayers.^{10,15}

Characterization of Capsules. Amphiphiles were proved by X-ray diffraction analysis and electron microscopy to exist as multiple bilayer structures in the porous capsule membrane.^{10,13,15,17} Thus, X-ray analysis of the intersection of the amphiphile-corked capsule showed strong reflections with 3.0–4.0-nm spacing, consistent with the bimolecular length of the amphiphile, depending on the alkyl chain length of the amphi-

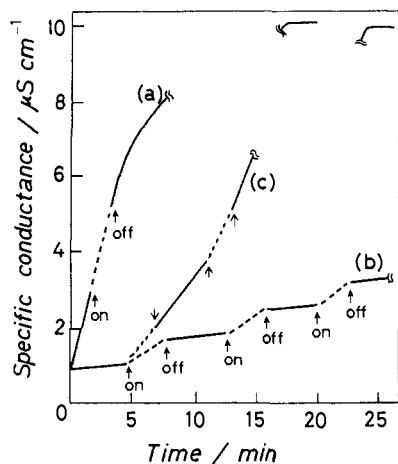


Figure 2. Electrically induced permeability control of NaCl through capsule membranes at 25 °C: (a) the uncorked capsule under a 60-V field; (b) the anionic $2C_{12}PO_4^-$ -corked capsule under a 60-V field; (c) the anionic $2C_{12}PO_4^-$ -corked capsule under a 100-V field. The external voltage source was applied at *on* and ceased at *off*.

philes. In transmission electron microscopy (a Hitachi H-500 instrument), the enlargement of a favorable area of an ultrathin piece of the amphiphile-corked capsule membrane (negatively stained by uranyl acetate) showed the distinct lamellar structure, the mean thickness of which is estimated to be 3.0–4.0 nm. These results clearly indicate that the corking amphiphiles exist as a multilamellar structure growing parallel to the membrane plane (illustrated in Figure 1).

Differential scanning calorimetry (DSC) was carried out with a Seiko Electric Co. Model SSC-575 instrument. Five crushed, bilayer-corked capsules were sealed with 50 μ L of water in an Al-sample pan and heated from 5 to 90 °C at 5 °C per min. All the amphiphiles on the capsule membrane showed a sharp endothermic peak, which indicates a phase transition from crystal to liquid crystal state, similar to that shown in aqueous dispersions of bilayer vesicles.¹⁹ Phase transition temperatures (T_c) obtained from a peak top of DSC curves were as follows: the cationic $2C_nN^+2C_1$, 10 °C ($n = 12$), 25 °C ($n = 14$), 38 °C ($n = 16$), 45 °C ($n = 18$); the anionic $2C_{12}PO_4^-$, 45 °C; the zwitterionic $2C_{16}PC$, 51 °C.

Measurements. The intermittent exposure of an external electric field to the capsule was performed by the apparatus shown in Figure 1; the capsule was placed between two platinum electrodes (area 1 cm \times 1 cm; separation between two electrodes 1 cm) connected to a high-voltage power supply (dc 0–300 V).

Permeation of NaCl or glucose was followed by detecting increases in the electrical conductance or glucose concentration, respectively, after dropping one capsule into the distilled water as shown in apparatus A of Figure 1. Glucose concentration was measured by detecting hydrogen peroxide with the H_2O_2 electrode covered with a glucose oxidase (GOD) fixed film. Permeation of water-soluble dyes was detected spectrophotometrically at 250 nm with use of apparatus B.

Apparent permeation rates P ($cm\ s^{-1}$) were calculated from eq 1,^{8–17}

$$P = \frac{1}{6} \frac{kd}{C_0} \quad (1)$$

where k and d are the increases in the permeant concentration of the outer phase with time (an initial slope) and the capsule diameter, respectively. C_0 is the concentration of probes trapped in the inner aqueous phase. Permeation measurements were carried out at least in triplicate in the individual conditions with or without an electric field and gave good reproducibility. The P values obtained showed $\pm 5\%$ deviation.

Results

Permeation of NaCl. Permeation of NaCl trapped in the inner aqueous phase of the capsule to the outer aqueous phase was measured by detecting increases in electrical conductance of the outer medium. Figure 2 shows typical time courses of the NaCl leakage under the intermittent electric field. In the case of the uncorked, semipermeable capsule, the permeation was very fast [$P = (1.88 \pm 0.09) \times 10^{-5} cm\ s^{-1}$] and not affected by the external voltage (20–100 V). In contrast, when the anionic $2C_{12}PO_4^-$ bilayer-corked capsule membrane was employed, the permeation of NaCl was reduced markedly because of a high barrier of the corking bilayers to permeability [$P = (7.12 \pm 0.36) \times 10^{-7} cm$

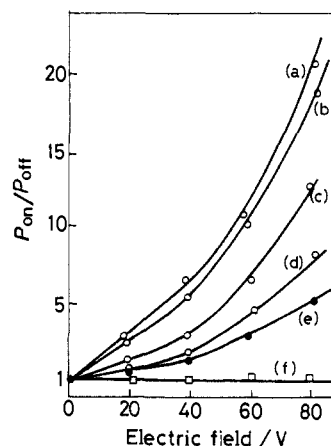


Figure 3. Effect of alkyl chain length of $2C_nN^+2C_1$ ($n = 12$ –18)-corked capsule membranes on the NaCl permeation under the electric field from 0 to 80 V at 25 °C: (a) $n = 18$; (b) $n = 16$; (c) $n = 14$; (d) $n = 12$; (e) $n = 18$ at 60 °C; (f) the uncorked capsule.

s^{-1}). The permeability was enhanced 10 times [$P = (7.21 \pm 0.36) \times 10^{-6} cm\ s^{-1}$] under a 60-V field, relative to that in the absence of the electric field. When the electric field ceased even after a long charging duration (3–5 min), the permeability reverted to the original slow rate [$P = (7.30 \pm 0.40) \times 10^{-7} cm\ s^{-1}$]. This permeability change could be reproduced repeatedly without damaging either corking bilayers or nylon capsule membranes. The similar electrically induced permeation enhancement was observed in the case of the capsule corked with the cationic $2C_{18}N^+2C_1$ or the zwitterionic $2C_{16}PC$ bilayers. This indicates that the effect of the electric field is independent of a surface charge of the corking bilayers. The effect of a temperature increase or electrolysis during experiments was negligibly small under the conditions employed.

The extent of the rate enhancement under the electric field (P_{on}/P_{off}) was exponentially increased with increasing electric field in a range of 0–80 V. On applying the voltage above 100 V or increasing the charging duration beyond 10 min, the NaCl leakage did not revert to the original slow rate, probably because of the rupture of the bilayer structure, as shown in curve c of Figure 2.

The effect of the strength of the applied electric voltage on the rate enhancement (P_{on}/P_{off}) of the capsule corked with the cationic $2C_nN^+2C_1$ bilayers ($n = 12$ –18) is shown in Figure 3. P_{on}/P_{off} values of the $2C_nN^+2C_1$ -corked capsule membrane were increased with increased external electric field in a range of 0–80 V, in contrast to those of the uncorked, semipermeable capsule membrane. The extent of the rate enhancement largely depended on the alkyl chain length of $2C_nN^+2C_1$ bilayers; the P_{on}/P_{off} value of $2C_{18}N^+2C_1$ - or $2C_{12}N^+2C_1$ -corked capsule membrane was 20 or 8 under a 80-V field, respectively. When the $2C_{18}N^+2C_1$ -corked capsule ($T_c = 45$ °C) was employed at 60 °C, the effect of the electric field was very small, relative to that at 25 °C. Phase transition temperatures (T_c) of the $2C_nN^+2C_1$ bilayers are 45, 38, 25, and 10 °C for $n = 18, 16, 14,$ and 12, respectively. At 25 °C, the $2C_{18}N^+2C_1$ and $2C_{16}N^+2C_1$ bilayers are in the rigid solid state below T_c , and the effect of the electric field on the permeation is larger than that for the $2C_{14}N^+2C_1$ and $2C_{12}N^+2C_1$ bilayers in the fluid liquid crystalline state above T_c . The similar temperature effect was observed for the capsule corked with anionic $2C_{12}PO_4^-$ bilayers ($T_c = 45$ °C); the effect of the electric field on permeation was 2.5 times larger at 25 °C (below T_c) than at 60 °C (above T_c). These results demonstrate that the permeability enhancement appears clearly in the solid state of corking bilayers in comparison with the fluid liquid crystalline state.

Permeation of Glucose and $CaCl_2$. It should be considered whether the electroanalysis is effective for the rate enhancement induced by the electric field in the NaCl permeation or not. Na^+ and Cl^- ions may be drawn to a cathode and an anode by electrostatic forces, respectively, and the permeability consequently

Table I. Effect of the Strength of the Electric Field on the Permeation Rate of NaCl, CaCl₂, and Glucose at 25 °C^a

electric field	$P/10^{-7} \text{ cm s}^{-1}$					
	uncorked capsule			2C ₁₈ N ⁺ 2C ₁ -corked capsule		
	NaCl	CaCl ₂	glucose	NaCl	CaCl ₂	glucose
0	188 (1.0)	133 (1.0)	52.0 (1.0)	8.7 (1.0)	5.3 (1.0)	1.0 (1.0)
20	210 (1.1)	148 (1.1)	54.0 (1.0)	24.2 (2.8)	15.0 (2.9)	3.0 (3.0)
40	202 (1.1)	186 (1.4)	57.2 (1.1)	36.7 (4.2)	20.5 (3.9)	4.5 (4.5)
60	228 (1.2)	152 (1.2)	62.4 (1.2)	47.8 (5.5)	26.1 (5.0)	7.0 (7.2)
80	237 (1.3)	183 (1.4)	63.0 (1.2)	93.6 (11)	53.0 (10)	12.5 (12)

^a P values contain the $\pm 5\%$ experimental errors. Numbers in parentheses show the permeation rate enhancement under an electric field ($P_{\text{on}}/P_{\text{off}}$).

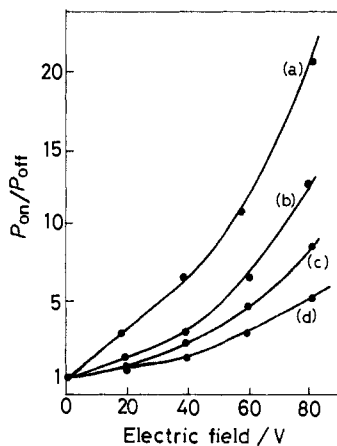


Figure 4. Effect of the conductivity of the corking bilayers on the electrically induced permeability enhancement of NaCl at 25 °C: (a) the capsule corked solely with 2C₁₈N⁺2C₁ bilayers; (b, c, d) the capsules corked with 2C₁₈N⁺2C₁ bilayers containing 17%, 34%, and 50% of di-4-ASP molecules, respectively.

increases under the electric field. In order to elucidate the effect of the electrostatic force, permeation of glucose as a neutral substance and CaCl₂ as a divalent cation was investigated with or without the electric field and the results are summarized in Table I. The obtained P values contain $\pm 5\%$ experimental errors. When the uncorked capsule was employed, permeation of glucose and CaCl₂ was fast and hardly affected by the electric voltage ranging between 0 and 80 V, as well as that of NaCl. In the case of the 2C₁₈N⁺2C₁-corked capsule membrane, permeation of neutral glucose and divalent CaCl₂ ions was enhanced under the electric field, depending proportionally on its strength, and the extent of the rate enhancement among NaCl, neutral glucose, and divalent CaCl₂ was almost the same. Thus, the electrostatic force between permeants and electrodes is not important for the electrically induced permeability enhancement.

Glucose seems to be less permeable (ca. 0.1–0.4 times) than NaCl and CaCl₂ from the bilayer-corked capsule both in the absence and in presence of the electric field (see Table I). In lipid bilayer vesicles (liposomes), glucose is approximately 1000 times more permeable than NaCl and this is explained by the relatively hydrophobic glucose compared with the hydrated NaCl. The permeability of the bilayer-corked capsule seems to be determined by the molecular size but not the hydrophobicity or the hydration of permeants, and small NaCl can permeate through bilayers more readily than relatively large glucose or naphthalene probes. This different behavior of permeability may be explained by the different bilayer structures of bilayer-corked capsules and liposomes: the capsule is corked with multiple, fragmented lamella bilayers (see Figure 1) and the wall of liposomes is composed of complete single (or multiple) bilayers.

Conductivity of Corking Bilayers. When a strong electric field was submitted from both sides of the bilayer-corked capsule membrane, the corking bilayers can be regarded as a capacitor because of the poor conductivity of lipid bilayers. The conductivity of bilayers may be important to cause the permeation rate enhancement under the electric field. Figure 4 shows the effect of the electric field of NaCl permeation when the high conductive molecule di-4-ASP was incorporated into the bilayers. The di-

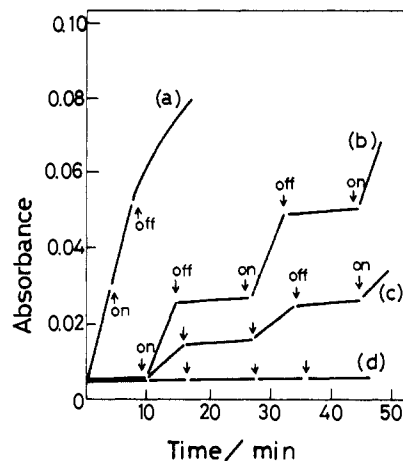
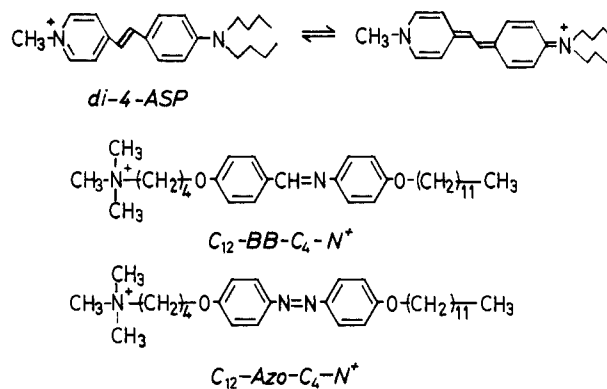


Figure 5. Electrically induced permeability enhancement of water-soluble dyes through the 2C₁₂PO₄⁻-corked capsule membrane at 50 °C: (a) the dianionic naphthalene probe 4 through the uncorked capsule; (b) the dianionic naphthalene probe 4; (c) the nonionic naphthalene probe 1; (d) the tetraanionic pyrene probe 6. A 20-V electric field was applied at *on* and ceased at *off*.

4-ASP, 4-(*p*-dibutylaminostyryl)-1-methylpyridinium bromide, which is well-known for the electrochromic molecular probe of the membrane potential,^{18,20,21} is expected to increase the conductivity of bilayers because of the large charge distributing down to the long axis of the chromophore under the electric field. The



extent of the rate enhancement decreased with increasing the content of di-4-ASP molecules in lipid bilayers; the $P_{\text{on}}/P_{\text{off}}$ value at a 80-V field was only 5 in the capsule corked with bilayers containing 50 wt% di-4-ASP molecules, in contrast to $P_{\text{on}}/P_{\text{off}} = 20$ in the capsule corked solely with lipid bilayers. When the bilayer-forming amphiphile having a dipole moment,²² C₁₂-BB-C₄-N⁺ or C₁₂-Azo-C₄-N⁺, was incorporated into the corking bilayers, the $P_{\text{on}}/P_{\text{off}}$ value was also decreased relative to that of the capsule corked solely with 2C₁₈N⁺2C₁ bilayers, although the extent was small. These results indicate that the corking bilayers act as a capacitor, and a high electric resistance of lipid bilayers is important for charging the large transmembrane potential.

Permeation of Large Molecules. When the relatively large substances such water-soluble naphthalene molecules were employed as a permeant, similar rate enhancement could be observed under the electric field. Figure 5 shows typical time courses of

Table II. Permeation Rates of Water-Soluble Dyes with or without the 20-V Electric Field at 50 °C^a

permeant	$P/10^{-7} \text{ cm s}^{-1}$					
	uncorked capsule			$2\text{C}_{12}\text{PO}_4^-$ -corked capsule		
	off	on	$P_{\text{on}}/P_{\text{off}}$	off	on	$P_{\text{on}}/P_{\text{off}}$
nonionic naphthalene 1	80.0	84.0	1.0	1.01	12.5	12
zwitterionic naphthalene 2	58.2	59.0	1.0	1.80	18.5	10
monoanionic naphthalene 3	298	300	1.0	2.5	110	44
dianionic naphthalene 4	179	185	1.1	2.7	190	71
trianionic naphthalene 5	135	150	1.1	1.0	176	176
tetraanionic pyrene 6	12	12	1.0	3.0	3.0	1.0

^a P values contain the $\pm 5\%$ experimental errors. Off and on mean permeation rates with and without an electric field, respectively.

Table III. Permeation Rates of the Nonionic Probe **1** across the $2\text{C}_{12}\text{PO}_4^-$ -Corked Capsule Membrane in the Presence of NaCl under the 20-V Electric Field at 50 °C^a

NaCl concentration	$P/10^{-7} \text{ cm s}^{-1}$		
	off	on	$P_{\text{on}}/P_{\text{off}}$
in the inner aqueous phase			
none	1.01	12.5	12
$1 \times 10^{-3} \text{ M}$	1.05	4.20	4.0
$1 \times 10^{-2} \text{ M}$	1.08	2.50	2.3
in the outer aqueous phase			
none	1.01	12.5	12
$1 \times 10^{-5} \text{ M}$	1.18	22.8	19
$5 \times 10^{-5} \text{ M}$	1.09	48.5	44

^a P values contain the $\pm 5\%$ experimental errors.

permeation of water-soluble dyes across the $2\text{C}_{12}\text{PO}_4^-$ -corked capsule membrane under a 20-V electric field. Permeation of the naphthalene probes **1** and **4** could be repeatedly controlled by the electric field as well as that of NaCl, CaCl_2 , and glucose, and the effect of the rate enhancement of the anionic probe **4** was larger than that of the nonionic probe **1**. When the large pyrene probe **6** was used for a permeant, however, the permeability was hardly affected by the electric field.

The permeation rates of various water-soluble probes with or without the 20-V field are summarized in Table II, in order to study the effect of molecular size and the charge of permeants on the electrically induced rate enhancement. Permeation of all large probes through the uncorked, semipermeable capsule was very fast and hardly enhanced by the electric field, independent of the molecular size and the charge of probes. When the $2\text{C}_{12}\text{PO}_4^-$ -corked capsule membrane was employed, permeation of the neutral naphthalene molecule **1** and **2** was enhanced 10–12 times under 20-V fields relative to that in the absence of the electric field. In the case of anionic naphthalene molecules, however, the permeation was largely enhanced in the order of mono-, di-, and trianionic probes even under the weak 20-V electric field; the $P_{\text{on}}/P_{\text{off}}$ value of the trianionic probe **5** amounted to 176. On the contrary, when the tetraanionic pyrene probe **6** was employed, the permeability was not enhanced probably because of the two times larger molecular size of the pyrene probe than that of the naphthalene probe.

Effect of Ionic Strength. The ionic strength of the outer and inner aqueous phase will affect the strength of the electric field across a capsule membrane between two electrodes. Permeation rates of NaCl as a small permeant and the nonionic probe **1** through the $2\text{C}_{12}\text{PO}_4^-$ -corked capsule membrane in the presence of NaCl in the inner or outer aqueous phase are summarized in Table III. The $P_{\text{on}}/P_{\text{off}}$ value was decreased with increasing NaCl concentration in the inner aqueous phase of the capsule. On the contrary, when the NaCl existed in the outer aqueous phase, the electrically induced permeability enhancement was largely increased.

Effect of Temperature, Arrhenius Plots. The phase transition from a solid-like state to a liquid crystalline state is one of the fundamental physicochemical properties of lipid bilayers. Permeation rates of NaCl as a small permeant and the nonionic probe **1** as a large permeant were obtained with or without the electric field at temperatures below and above T_c , and Arrhenius plots are shown in Figures 6 and 7, respectively. In the case of the uncorked capsule, both permeants gave the simple, straight plots.

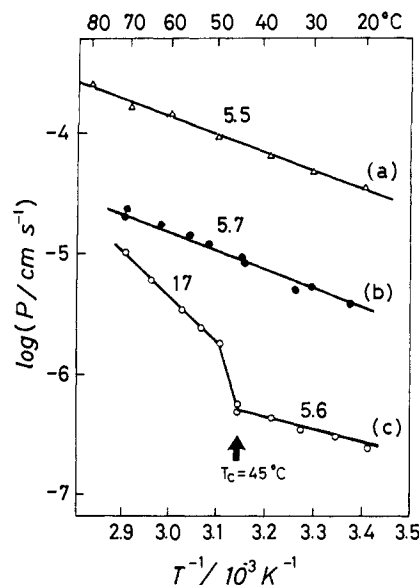


Figure 6. Arrhenius plots of NaCl permeation through capsule membranes: (a) the uncorked capsule; (b) the $2\text{C}_{12}\text{PO}_4^-$ -corked capsule under a 60-V electric field; (c) the $2\text{C}_{12}\text{PO}_4^-$ -corked capsule in the absence of the electric field. Numbers are the activation energies (E_a , kcal mol⁻¹) obtained from the slopes. The arrow shows T_c of the corking $2\text{C}_{12}\text{PO}_4^-$ bilayers as obtained from DSC measurements.

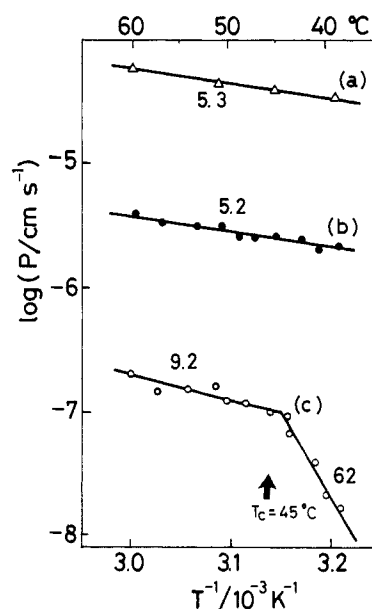


Figure 7. Arrhenius plots of the permeation of the nonionic naphthalene probe **1** through capsule membranes: (a) the uncorked capsule; (b) the $2\text{C}_{12}\text{PO}_4^-$ -corked capsule under a 20-V electric field; (c) the $2\text{C}_{12}\text{PO}_4^-$ -corked capsule in the absence of the electric field. Numbers are E_a values (kcal mol⁻¹).

In the absence of the electric field, the $2\text{C}_{12}\text{PO}_4^-$ -corked capsule gave a drastic inflection near T_c of the corking bilayers ($T_c = 45$

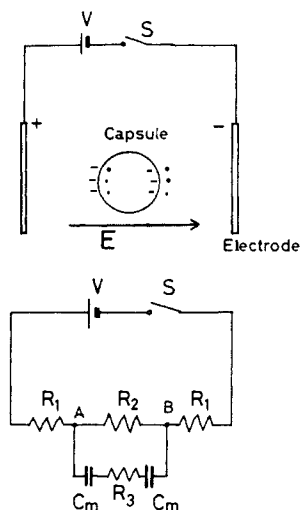


Figure 8. Schematic representations of the electric field across the bilayer-corked capsule membrane and a model circuit diagram. R_1 and R_2 , resistances of the outer aqueous phase; R_3 , the resistance of the inner aqueous phase; C_m , the capacitance of the bilayer-corked capsule membrane ($1\text{-}\mu\text{m}$ thick); V , voltage source.

$^{\circ}\text{C}$) because of the phase transition from the rigid solid-like state to the fluid liquid crystalline state. Under the influence of the electric field, the permeation of NaCl and the probe **1** was accelerated 3–15 times compared with that in the absence of the electric field over the whole temperature range, and Arrhenius plots hardly inflected near T_c . The larger rate enhancement was observed at temperatures below T_c than above T_c . This is consistent with the result of the temperature and alkyl chain length effects of the $2\text{C}_{18}\text{N}^+2\text{C}_1$ -corked capsule membrane on the rate enhancement (see Figure 3). The numbers on graphs are the activation energies (kcal mol^{-1}) obtained from Arrhenius slopes below and above the T_c .

Discussion

When the bilayer-corked capsule membrane was placed in the strong external electric field between two electrodes, the corking bilayers are polarized because of the movement of ions along the electric field lines. As a consequence, the electrogenicity of the capsule is severely perturbed. A schematic circuit diagram of the experimental setup is shown in Figure 8. Under the electric field, the corked bilayers on the capsule membrane can be regarded as two plate capacitors of specific conductance, C_m , because of the poor conductivity of lipid bilayers. The electrical breakdown would occur preliminary at the poles (that is, in the direction of the field) of the capsule and then spread in other areas of the membrane. When the 60-V electric field is applied between two electrodes, the electric potential between A and B (the horizontal diameter of a capsule) is estimated to be 12 V because the capsule diameter is one-fifth of a distance of two electrodes (1 cm). The transmembrane potential of each membrane ($1\text{-}\mu\text{m}$ thick) is calculated to be 6 V (corresponding to 60 kV cm^{-1}). The corking bilayers exist as a multilamellar structure on the capsule, so that the transmembrane potential per one bilayer (thickness, 5 nm) can be estimated to be 30 mV. In the electrical charge pulse experiments on liposomes or planar lipid bilayer membranes the reversible permeation enhancement by the electrical breakdown is observed when the membrane potential of 100–800 mV per lipid bilayer or the external electric field about $2\text{--}30\text{ kV cm}^{-1}$ was applied in a short duration (at $1\text{--}20\text{-}\mu\text{s}$ range).^{3–7} These experiments are conclusive of the electric field induced transient pores in lipid bilayers.

We also tried to apply the pulse electric field of $10\text{--}100\text{ kV cm}^{-1}$ for $5\text{--}50\text{ }\mu\text{s}$ to a capsule between two electrodes as well as liposomal membranes. However, the permeability enhancement was hardly observed. We suppose that the pulse electric field in a short duration is not effective to cause the electric breakdown of multiple bilayers on the capsule membrane, unlike the single-wall bilayer vesicles, and the long charging duration over 1 min is required

to disturb multi-bilayers on the capsule.

For the induction of the electrical breakdown, the membrane should have the low conductivity in order to charge up potentials. A specific resistance of lipid bilayers is estimated to be in the order of $10^6\text{--}10^8\text{ }\Omega\text{ cm}^{-2}$, which is three to four orders of magnitude higher than that of the cell membrane.⁴ When the charge distributed chromophore, di-4-ASP, was embedded in the corking bilayers, the effect of the electric field on the permeability was decreased with increasing content of di-4-ASP molecules (see Figure 4). The incorporation of the di-4-ASP reduced the resistance of bilayers and the electrical breakdown hardly occurred in such a conductive bilayer. This clearly indicates that the corking bilayers act as a capacitor to charge the transmembrane potential under the electric field.

When electrolytes existed in the inner and the outer aqueous phase of the capsule, the electrically induced permeation enhancement of dyes was decreased and increased, respectively (see Table III). When electrolytes incorporated in the inner aqueous phase of the capsule with dyes, the small electrolyte can permeate first in order to reduce the membrane potential and the permeation of the large dye is not very enhanced under the electric field. In contrast, when electrolytes were in the outer aqueous phase, the apparent strength of the electric field increases because of the high conductivity of the outer aqueous phase. This effect is equivalent to reducing the distance between two electrodes.

The permeation mechanism in the absence of the electric field can be explained as follows,^{8–10} using the activation energy data in Figures 6 and 7. In the permeation of NaCl and dyes through the uncorked, semipermeable capsule membrane, Arrhenius plots gave a simple straight line with $E_a = 5.3\text{--}5.5\text{ kcal mol}^{-1}$, in which permeation mainly proceeds by diffusion. In permeation of small molecules such as NaCl through the bilayer-corked capsule membrane, NaCl permeates through the fluid, although the hydrophobic bilayer matrix has a relatively high activation energy ($E_a = 17\text{ kcal mol}^{-1}$) at temperatures above T_c (Figure 6). When the bilayer is in the rigid solid-like state below T_c , permeation through the bilayer matrix becomes difficult, and NaCl permeates slowly through defective pores in the multilamellar structures instead. The E_a value below T_c (5.6 kcal mol^{-1}) then becomes similar to that of the uncorked capsule membrane (5.5 kcal mol^{-1}). For the permeation of the relatively bulky molecule such as the probe **1** through the rigid solid-like bilayers below T_c , the permeant cannot pass through the small defective pores in lamellae and must diffuse, disturbing or melting a large number of boundary lipids in bilayers with a very high E_a value (62 kcal mol^{-1}) (Figure 7). At temperatures above T_c , the probe **1** can permeate through the fluid liquid crystalline bilayers with a small E_a value (9.2 kcal mol^{-1}).

Under the influence of the electric field, the permeation of both NaCl and the probe **1** was accelerated 3–15 times compared with that in the absence of the electric field over the whole temperature range, and the Arrhenius plot gave a simple straight line without inflections near T_c . E_a values of both permeants under the electric field are small ($5.2\text{--}5.7\text{ kcal mol}^{-1}$) and nearly equal to that in permeation through the uncorked capsule membrane or that in permeation of NaCl through the defective pores in solid-state bilayers in which the permeants pass through pores by a diffusion process. This suggests that the transmembrane potential induced by the electric field generates many transient pores or distortions in the corking bilayers and NaCl or dyes pass rapidly through these pores with a small activation energy. The permeability was enhanced 3–15 times under the electric field; however, it is still 10 times less than that of the uncorked capsule. This indicates that transient pores form partially (e.g., at the poles in the direction of the field), but not the whole part of the bilayer corkings. When the extremely high voltage ($>120\text{ V}$) was applied to the capsule, the permeability approached nearly to that of the uncorked capsule and did not revert to the original slow rate when the electric field was turned off because of the rupture of the bilayer structure.

Although permeation of NaCl, glucose, and up to water-soluble naphthalene molecules was enhanced under the electric field, permeation of the much larger pyrene molecule **6** was not affected

at all (see Table II). Thus, transient pores induced by the electrical breakdown are permeable to the molecular size up to naphthalene molecules but not to the large pyrene molecules. In the pulsation experiments of the planner lipid bilayer membranes, it is reported that the number of transient pores created during a short duration of the electrical breakdown is estimated to be $10^7/\text{cm}^2$, and the pore radius is calculated to be 4 nm.²³

Molecular mechanisms responsible for the opening of transient pores are not yet clear. One may consider²⁴ that polar head groups of lipids are reoriented, which allows a rapid leakage of permeants under the electric field. When the bilayer is assumed to be elastic but incompressible,²⁵ the applied field induces a stress on the lipid bilayer and thins down the membrane. Consequently, the area per lipid must increase and such an expansion of the bilayer membrane may be responsible for the transient pores. Another interpretation of these pores is given by the analysis of electrical breakdown of planner lipid bilayers.²⁶ In that case, spontaneous pores exist in the membrane due to the structural defects whose development is favored by the electric field.

(23) Benz, R.; Zimmermann, U. *Biochim. Biophys. Acta* **1981**, *640*, 169.

(24) Seeling, J. *Q. Rev. Biophys.* **1977**, *10*, 353.

(25) White, S. H. *Biophys. J.* **1974**, *14*, 155.

(26) Abidor, I. G.; Arakelyan, V. B.; Chernomordish, L. V.; Chizmadzhev, Yu. A.; Pastushenko, V. F.; Tarasevich, M. R. *Bioelectrochem. Bioenerg.* **1979**, *6*, 37.

Summary

Although nylon capsule membranes were simply semipermeable, the capsule corked with lipid bilayers could reversibly regulate the permeability by the external electric field. The transient pores induced by an electrical breakdown are reversibly generated for a long duration (3–5 min) in the corking bilayers and have a selectivity for the dye permeation. It is difficult, however, for liposomal membranes to realize the reversible permeation control and form transient pores for any long duration, because they are easily damaged or fused each other under the electric field. On the contrary, the bilayer-corked capsule membrane is not damaged by the continuous and intermittent electric field, because lipid bilayers are supported by the physically strong nylon capsule wall. The signal receptive permeability control induced by the electric field is reproducible and useful for a model of the synaptic systems in which a nerve electrical impulse initiates the rapid release of a chemical intermediary.

Registry No. 1, 97732-71-3; 2, 99646-32-9; 3, 130-14-3; 4, 1655-29-4; 5, 5182-30-9; 6, 59572-10-0; di-4-ASP, 101630-71-1; $2\text{C}_{12}\text{N}^+2\text{C}_1$, 3282-73-3; $2\text{C}_{14}\text{N}^+2\text{C}_1$, 68105-02-2; $2\text{C}_{16}\text{N}^+2\text{C}_1$, 70755-47-4; $2\text{C}_{18}\text{N}^+2\text{C}_1$, 3700-67-2; $2\text{C}_{12}\text{PO}_4^-$, 45300-74-1; $2\text{C}_{16}\text{PC}$, 18545-88-5; $\text{C}_{12}\text{-BB-C}_4\text{-N}^+$, 101630-72-2; $\text{C}_{12}\text{-Azo-C}_4\text{-N}^+$, 101630-73-3; NaCl, 7647-14-5; CaCl_2 , 10043-52-4; *p*- $\text{Bu}_2\text{NC}_6\text{H}_4\text{CHO}$, 90134-10-4; D-glucose, 50-99-7; 4-picolinium, 16950-21-3; nylon-2,12, 41510-72-9; nylon-2,12 SRU, 41724-60-1.

Forces between Surfaces of Block Copolymers Adsorbed on Mica

Georges Hadziioannou,*† Sanjay Patel,† Steve Granick,†† and Matthew Tirrell*†

Contribution from the IBM Almaden Research Center, San Jose, California 95120, and the Department of Chemical Engineering and Materials Science, University of Minnesota, Minneapolis, Minnesota 55455. Received September 9, 1985

Abstract: Forces exerted between block poly(vinyl-2-pyridine)/polystyrene (PV2P/PS) copolymer layers adsorbed on mica substrates have been measured over the separation range 0–200 nm between the substrate surfaces. The PV2P block binds strongly to mica in a flattened configuration; the PS block is not bound directly to mica in our experiments. The PS block is held on the surface through its covalent bond to PV2P. The form and range of the force vs. separation curve depend upon block molecular weights and the thermodynamic quality of the immersion solvent for the PS chain. In the good solvent toluene, the PS chains are shown to be stretched away from the surfaces in extended configurations and to exert long-ranged, mutually repulsive forces when two layers are brought to a separation causing overlap of the PS chains. In the θ solvent cyclohexane, the range is reduced considerably due to configurational contraction and due to the diminished effects of binary interactions between polymer segments. The range of the forces observed and their dependence on block molecular weights can be explained by fairly simple arguments about the packing of polymer chains on the surface.

Conformations of macromolecules adsorbed on solid surfaces immersed in solvent are, in general, altered significantly from conformations of polymers dissolved in the bulk of the solvent.² Instrumental tools available to study these conformations are limited in both number and capability. Ellipsometry gives a characteristic thickness and mean refractive index of an adsorbed layer on a reflective substrate.³ Hydrodynamic measurements give a different characteristic length scale of the adsorbed configuration.⁴ Neutron scattering⁵ and fluorescence excited by evanescent waves through surfaces⁶ promise to provide more complete data on the polymer segment density profile within adsorbed layers but at present are fraught with complexities in interpretation. Detailed understanding of the conformations of adsorbed macromolecules rests upon knowledge of the intermolecular forces between polymers and solid substrates and on how these forces are affected by environmental conditions such as

temperature and the thermodynamic quality of the immersion solvent.

(1) Permanent address: Polymer Group and Department of Ceramic Engineering, University of Illinois, Urbana, IL 61801.

(2) Takahashi, A.; Kawaguchi, M. *Adv. Polym. Sci.* **1982**, *46*, 1. This reference presents an excellent review of all experimental and theoretical results on the configurations of adsorbed polymers. Such a comprehensive review is therefore omitted from the current article.

(3) Kawaguchi, M.; Takahashi, A. *J. Polym. Sci., Polym. Phys. Ed.* **1980**, *18*, 2069.

(4) (a) Priel, Z.; Silberberg, A. *J. Polym. Sci., Polym. Phys. Ed.* **1978**, *16*, 1917. (b) Varoqui, R.; Dejardin, P. *J. Chem. Phys.* **1977**, *66*, 4395.

(5) (a) Barnett, K. G.; Cosgrove, T.; Vincent, B.; Burgess, A. N.; Crowley, T. L.; King, T.; Turner, J. D.; Tadros, T. F. *Polymer* **1981**, *22*, 283. (b) Barnett, K. G.; Cosgrove, T.; Vincent, B.; Sissons, D. S.; Cohen-Stuart, M. *Macromolecules* **1981**, *14*, 1018.

(6) (a) Allain, C.; Ausserré, D.; Rondelez, F. *Phys. Rev. Lett.* **1982**, *49*, 1694. (b) Ausserré, D.; Hervet, H.; Rondelez, F. *Macromolecules* **1986**, *19*, 85. (c) Ausserré, D.; Hervet, H.; Rondelez, F. *Phys. Rev. Lett.* **1985**, *54*, 1948. (d) Bloch, J. M.; Sansone, M.; Rondelez, F.; Peiffer, B. G.; Pincus, P.; Kim, M. W.; Eisenberger, P. *Phys. Rev. Lett.* **1985**, *54*, 1039.

* IBM Almaden Research Center.

† University of Minnesota.